Title:	Investigation of Luminescent Ceria as a Plutonium Oxide Simulant Final Report
Author(s):	Hargather, Chelsey Kimberley, Jamie Grow, David Isaac Krishnamoorthy, Wish Berg, Nathan Smith, Paul Herrick
Intended for:	General distribution to academic community
Issued:	2021-03-25

Investigation of luminescent ceria as a plutonium oxide simulant

Final Report

Drs. Chelsey Hargather*[1], Jamie Kimberley [2], Wish Krishnamoorthy [3], Nathan Berg [3], David Grow*[4], and Paul Smith*[4]
[1]New Mexico Tech, Dept. of Materials Engineering
[2]New Mexico Tech, Dept. of Mechanical Engineering
[3]Qynergy, Inc., Albuquerque, NM
[4]Los Alamos National Laboratory, Los Alamos, NM
*chelsey.hargather@nmt.edu

March 26, 2020

NEW MEXICO TECH
SCIENCE • ENGINEERING • RESEARCH UNIVERSITY

Contents

1 Purpose

Plutonium oxide powders from various production lines at Los Alamos National Laboratory are stored and transported in specially designed "SAVY-4000", "Hagan", or other containment systems. Cerium oxide powder has been used as a less-hazardous simulant powder for testing accidental release from these containers under various operational scenarios. This work investigates the development and use of fluorescent cerium oxide powders as a more easily detectable, and potentially quantifiable, simulant powder for plutonium oxide container systems.

2 Scope

Nine luminescent cerium oxide (ceria) powders, chemical formula CeO_2, were produced by either (i) blending LANLs reference ceria with a commercial phosphor or (ii) doping the ceria microstructure with europium during synthesis of the powder. The particle size, particle morphology, agglomeration characteristics, and flowability for each of the resulting powders were tested. The fluorescent properties of each powder were tested to determine the ideal absorption and emission ranges. The following bullet points summarize the methods used to characterize the nine powders:

- Scanning electron microscopy (SEM) was used to determine particle size and particle morphology.
- Tapping of the powders was performed to measure their volume changes make conclusions about their flowability and density characteristics by calculating associated tapped density.
- Ultraviolet and visible spectroscopy (UV-Vis) was used to show the complete absorption spectrum for all of the powders.
- Photoluminescence spectroscopy (PL) was used to determine the peak emission range for all of the powders.
- Brunauer-Emmett-Teller (BET) analysis was used to measure the surface area of the powder samples.
- Transmission electron microscopy (TEM) was performed to determine particle size and morphology of the various simulant powders.

Table 2.1 shows the names of and abbreviations for the powders that were characterized in the present work. RCe is the reference ceria supplied by LANL. Samples with an A, B, or C designation refer to blended samples, where a certain amount of commercial phosphor was blended with the reference ceria. Samples with the Eu designation refer to ceria powder that was doped with luminescent europium. The Eu samples were made by American Elements in accordance with the procedure found in the publication by Vimal et al. [1].

Table 2.1: Various powder samples characterized in the present work, with their abbreviations.

Abbreviation	Name
RCe	Reference cerium oxide
A1	Commercial Phosphor: G525 Green
A3	Ceria blended with 5 wt% G525
A4	Ceria blended with 2.5 wt% G525
B1	Commercial Phosphor: Y550 Yellow
B3	Ceria blended with 5 wt% Y550
B4	Ceria blended with 2.5 wt% Y550
C1	Commercial Phosphor: Y570 Yellow
C3	Ceria blended with 5 wt% Y570
C4	Ceria blended with 2.5 wt% Y570
Eu0.5	Ceria doped with 0.5 wt% Eu
Eu1	Ceria doped with 1 wt% Eu
Eu2	Ceria doped with 2 wt% Eu

3 Methodology

Various experimental procedures were used in the present work to characterize and compare the luminescent and non-luminescent ceria. Each procedure is described in detail below.

3.1 Optical Microscopy

1. A Hirox KH-7700 digital microscope was used for optical characterization of the A3, A4, B4, C3, Eu0.5, Eu1, and Eu2 powders.

2. Double-sided adhesive tape was placed on microscope slides, and a scoopula was used to apply a small amount of powder to create the sample specimens.

3. The excess powder was removed with tapping followed by a blast of canned air (computer duster).

4. Steps 2-3 were repeated until all samples were created for imaging.

5. Each sample was imaged using the Hirox KH-7700 digital microscope. Brightness and contrast were adjusted for each image individually.

3.2 Scanning Electron Microscopy (SEM)

1. A Hitachi S-4100 field emission scanning electron microscope (FE-SEM) was used to characterize the different powder samples. The samples that were imaged were the Eu0.5 doped powder, A4 blended powder, and RCe, the reference ceria oxide powder sample.

2. The preparation of the samples for imaging started with preparing the sample stand. Double sided carbon tape, was cut into unique and easily identifiable shapes and carefully placed, with sufficient separation, on a clean SEM sample stand.

3. All but one carbon tape section was covered with wax paper to avoid cross contamination.

4. The uncovered carbon tape was oriented below the covered sections and a scoopula was used to apply a small amount of powder sample to the carbon tape. The powder was lightly pressed into the tape to ensure adhesion.

5. The unsecured powder was removed by gently blowing with a purified air duster away from the other, still covered carbon tape sections. Then the wax paper was removed.

6. Steps 2 through 5 were repeated until samples of the reference RCe, Eu0.5 doped, and A4 blended had been prepared.

7. The samples were sputter coated with Pt using the EMITECH K950X sputter coater.

8. Several images were taken of each sample with a Hitachi S-4100 FE-SEM. Brightness and contrast were adjusted for each image individually.

3.3 Transmission Electron Microscopy (TEM)

1. Approximately 0.1g of RCe powder was suspended in ethanol.

2. A drop of the particle suspension was placed onto a holey carbon backed copper grid.

3. The ethanol was allowed to evaporate in ambient conditions, depositing the powder onto the holey carbon backed copper grid.

4. The sample was placed into the TEM machine for imaging.

5. The TEM analysis was done using a JEOL 2010F microscope at University of New Mexicos Center for Micro-Engineered Materials User Facility.

6. Steps 1-5 were repeated from the Eu0.5 sample.

3.4 Brunauer-Emmett-Teller (BET)

1. The Micromeretics ASAP 2010 system as shown in Figure 3.1 was used to perform the BET surface area measurements.

2. Reference ceria, RCe, was degassed under vacuum at 250 °C for 96 hours then the heat was turned off.

Figure 3.1: Micromeritics ASAP2010 BET Surface Area Analysis Instrument

3. Samples remained under vacuum for a total of 168 hours and had reached a base pressure of 1 mT prior to analysis.

4. 5-point analysis was run using N_2 as the adsorptive gas. The volume of gas adsorbed to the surface of the particles is measured at the boiling point of the analysis gas (-196 °C for nitrogen).

5. The equilibrium pressure and saturation pressure of the adsorbate at the temperature of adsorption are measured, as well as volume of adsorbed gas. Using the BET equation (described in detail in Section 4.2) the surface area of the sample is determined.

6. Steps 2-5 were repeated for 0.5% Eu doped ceria, Eu0.5.

3.5 Tapped Density Procedure

1. Samples of approximately 3 grams were prepared and weighed to a precision of 0.0001 g for the reference ceria (RCe) and each of the blended samples (A3, A4, B3, B4, C3, C4). Samples of approximately 1 gram were prepared and weighed to a precision of 0.0001 g for each of the europium powders (Eu0.5, Eu1, Eu2).

2. After one sample of powder was weighed, it was transferred to a 5 mL graduated cylinder with 0.1 mL markings. The volume of the untapped powder was recorded.

3. The graduated cylinder top was covered with a cap.

4. The graduated cylinder was transferred to a beaker stand that has a clamp attachment. The base of the clamp was adjusted to the height of 4.5 cm from the base of the weigh stand.

5. The loaded graduated cylinder was placed inside the two sides of the clamp. The clamp was loosely tightened around the graduated cylinder to ensure that the cylinder did not tip over when dropped. The testing setup was shown in Figure 3.2.

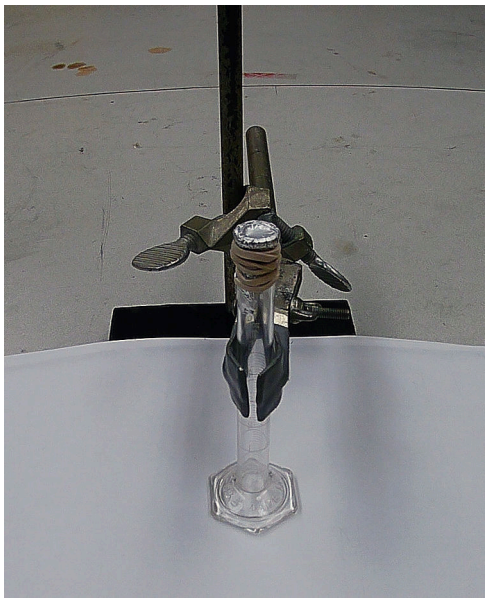

Figure 3.2: Testing setup for tap density tests.

6. The graduated cylinder was lifted to 4.5 cm from the base of the weigh stand and dropped repeatedly until volume of the powder remained constant.

7. The final, tapped, volume was recorded.

8. 5 trials were conducted for each powder sample, and the results were averaged together.

3.6 Spectroscopy Sample Preparation

1. 13 spectroscopy samples were prepared for the reference ceria, RCe, the pure commercial phosphors A1, B1, and C1, each of the blended samples, A3, A4, B3, B4, C3, and C4, and each of the doped samples Eu0.5, Eu1, and Eu2. The amount of powder varied from sample to sample due to the different powder densities and their different luminescent properties. The amount of each powder was selected for optimized results from the photometers. Too little powder would render the samples absorption or emission wavelength not detectable, and too much powder would overwhelm the machines and absorption or emission peaks were not able to be identified. Table 3.1 identifies the amount of powder used in each spectroscopy sample, weighed to a precision of 0.0001 g.

Table 3.1: Mass of each of the 13 powders used for creating the spectroscopy samples.

Powder type	Powder mass used in spectroscopy sample (g)
RCe	0.0024
A1	0.0331
B1	0.0312
C1	0.0320
A3	0.0042
A4	0.0023
B3	0.0023
B4	0.0025
C3	0.0028
C4	0.0043
Eu0.5	0.0012
Eu1	0.0010
Eu2	0.0043

2. The polydimethylsiloxane (PDMS) samples were weighed out to approximately 3.5 grams of PDMS and 0.35 grams of curing agent, with a precision of 0.0001 g.

3. The powder was mixed mechanically with the PDMS.

4. The mixed samples were cast in spectroscopy polystyrene cuvettes.

5. The cuvettes are placed in an 80 °C oven to heat cure for 40 minutes.

6. The oven was turned off to slow cool overnight. Figure 3.3 shows the 14 spectroscopy cuvettes created using this process.

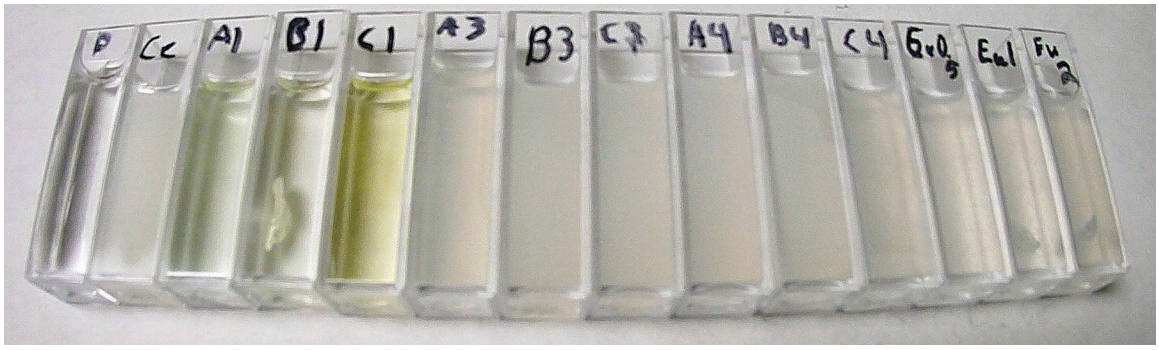

Figure 3.3: Cuvettes showing the powder samples suspended in PDMS.

7. Additionally, one reference sample of PDMS without power was cast according to steps 2, 4-7.

3.7 Ultraviolet-visible Spectroscopy (UV-Vis) Methodology

1. All sample cuvettes that were prepared according to the methodology of Section 3.6 were wiped down with a clean Kim-wipe.

2. Each sample was placed in a Beckman Coulter DU 720 UV-Vis spectrophotometer. The instrument is shown in Figure 3.4. The viewing sides of the cuvette were oriented towards the light path. (Note: Cuvettes have two clear viewing sides and two rough sides for handling.)

Figure 3.4: UV-Vis spectrometer used in the present work..

3. Each sample was scanned at wavelengths ranging from 300 nm to 790 nm.

4. The machine did not have adjustable integration speeds, as the machine scans to a user-specified resolution. For this work, the resolution was set to the maximum setting on the machine for the wavelength range indicated.

3.8 Flourospectroscopy

1. PDMS sample cuvettes that were prepared in Section 3.6 were wiped down with a clean Kim-wipe.

2. Each sample was placed in a Shimadzu RF-5301PC spectroflourophotometer, such that the beam path passes through the optical window for the full width of the cuvette. An image of the machine is given below in Figure 3.5.

3. Machine was set to excite the sample with the absorption peak wavelength determined from the UV-Vis measurements, $\pm$, 2.5 nm.

4. The emission mission slit width was maintained at 5 nm. The scans were performed in 1 nm increments.

Figure 3.5: Shimadzu RF-5301PC spectroflourophotometer

5. The spectrofluorophotometer was calibrated upon installation at NMT, and undergoes a self-calibration check before each scan. It is also periodically checked against reference samples for ensuring continued accuracy. Appendix A shows a recent calibration test using a standard coumarin 153 dye. When suspended in ethanol, coumarin 153 emits at 532 nm with a 422 nm excitation. The plot in Appendix A shows consistent emission from the spectrofluorophotometer at 532 nm of the dye in various amount of ethanol.

4 Results and Discussion

4.1 Particle Size Analysis

Optical microscopy, SEM analysis, and TEM analysis were performed on a variety of the blended and doped samples with two primary goals: (i) determine the particle and agglomerate sizes of each powder type and (ii) identify any interactions that occur in the blended samples between the ceria powder and the commercial phosphors.

4.1.1 Optical Microscopy

Imaging and discussion of the blended samples A4, B4, and C3 were considered first. Optical images of the C3 sample (RCe blended with the Y570 commercial phosphor) acquired under white light at different magnifications are shown in Figure 4.1.

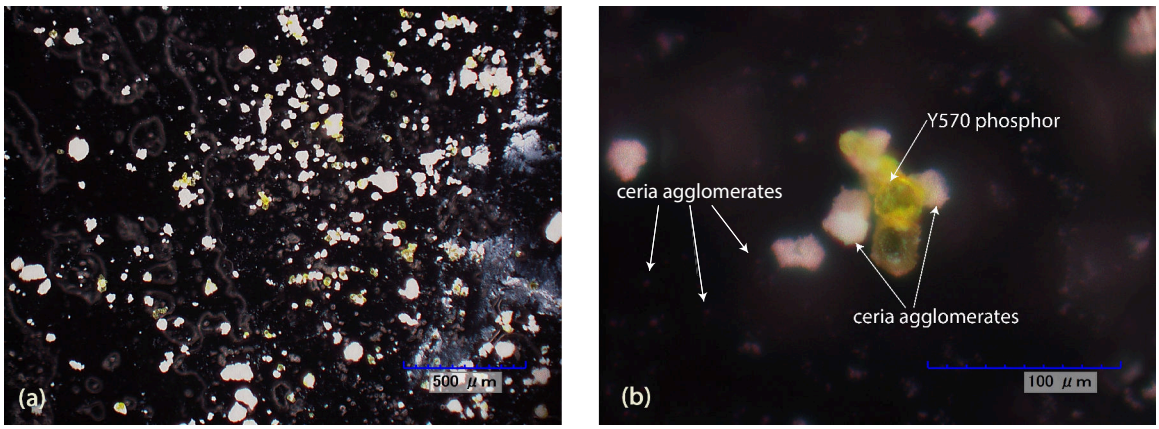

Figure 4.1: C3 blended sample showing (a) Y570 phosphor and ceria agglomerates at low magnification and (b) close up of the Y570 phosphors (yellow) surrounded by several ceria agglomerates.

In Figure 4.1 (a), the yellow Y570 particles are clearly visible in the micrograph and are dispersed with the reference ceria powder. The figure also demonstrates that the ceria agglomerates (white) span several orders of magnitude in size. Figure 4.1 (b) is a close up of several Y570 phosphor (clearly visible in yellow) particles surrounded by ceria agglomerates with sizes of the same order of magnitude. The commercial phosphors were similar in size to many of the ceria agglomerates. It is observed that individual phosphor particles are on the order of 10-12 μm. Figure 4.1 (b) shows substantially smaller ceria particles in the background of the image, indicating that the unagglomerated ceria particles may be several orders of magnitude smaller than the phosphor particles. Higher resolution microscopy such as SEM or TEM was needed to resolve the particle size of the individual ceria particles.

4.1.2 Scanning Electron Microscopy (SEM) Analysis

Scanning electron microscopy (SEM) imaging was performed on the A4 blended sample (G525 phosphor) using the Hitachi S-4100 FE-SEM. Figure 4.2 (a) shows a higher resolution image of a single G525 phosphor with ceria agglomerates of various size attached to it. The individual G525 phosphor particle is 10-12 μm in size, which is typical for this powder based on other SEM and optical observations. Figure 4.2 (b) shows that the primary particles of the ceria powder are significantly smaller than 1 μm and are likely smaller than 10 - 100 nm, but the individual ceria particles are too small to make exact size determinations using the FE-SEM.

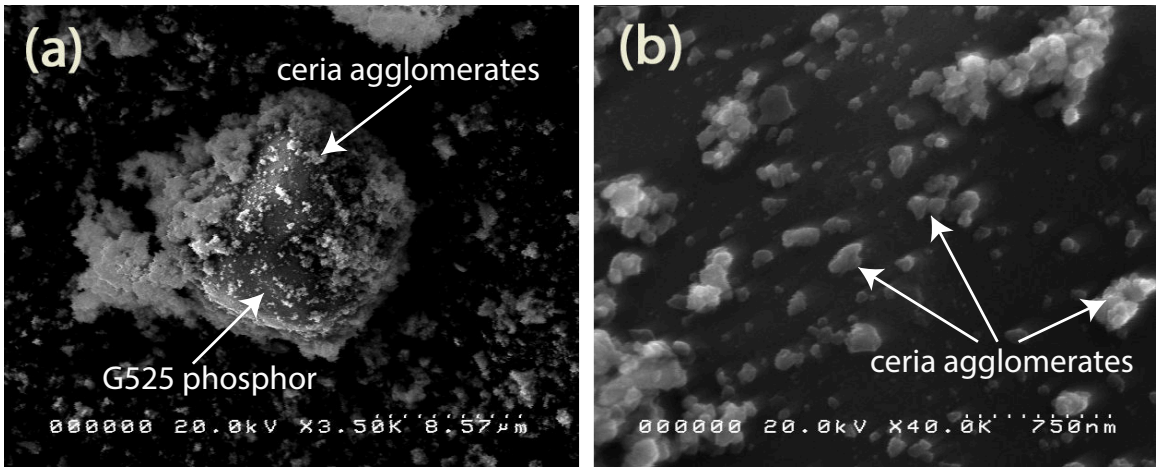

Figure 4.2: A4 blended sample showing (a) individual G525 phosphor particle with ceria agglomerates attached, (b) higher magnification of the powder showing ceria agglomerates

The FE-SEM images showing the size and structure of the doped sample Eu0.5 agglomerates are shown in Figure 4.3 (a) and (b). In terms of particle size of the doped ceria samples, Figure 4.3 (a) shows that agglomerate sizes range from 1 - 10 μm, while Figure 4.3 (b) demonstrates the presence of much smaller agglomerates/particles. Hence, TEM analysis was performed in Section 4.1.3 on these samples to better resolve the particle size. This difference in microstructure is understandable since the synthesis techniques employed for the reference Ceria are assumed to be different than that for the doped materials [1].

4.1.3 Transmission Electron Microscopy (TEM) Analysis

Transmission Electron Microscope (TEM) analysis was performed on undoped reference ceria, RCe, and doped Ceria, Eu0.5. The manufacturer specified that both powders had a median particle size of less than 1 micron. As mentioned in Section 4.1.2, the SEM analysis revealed that the particle sizes were too small to resolve.

The TEM analysis was performed using a JEOL 2010F microscope. The results from the TEM analysis on the reference ceria, RCe sample are shown in Figure 4.4. The RCe sample showed particles sizes in the 50-100 nm range, as shown in Figure 4.4 (a). The

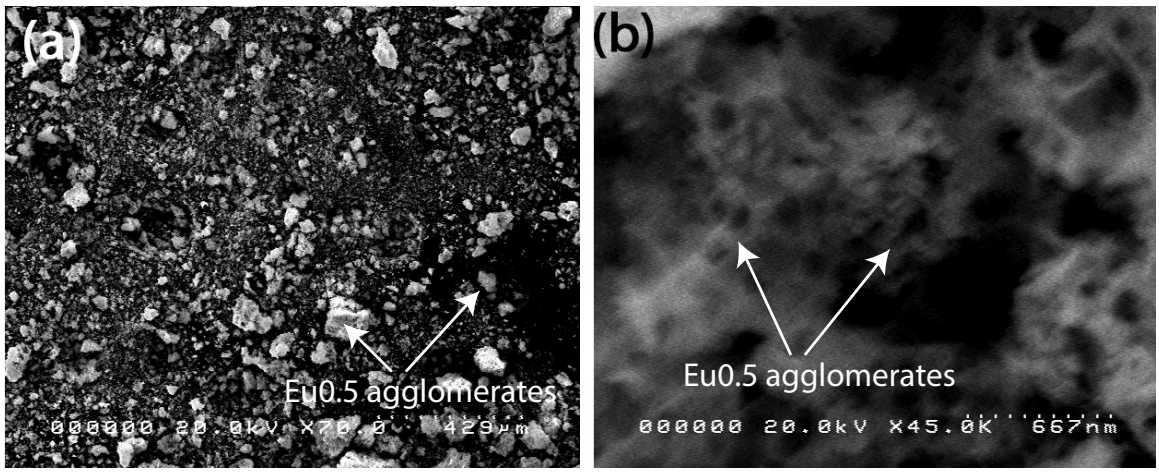

Figure 4.3: SEM images of the Eu0.5 sample agglomerate structure at (a) low magnification and (b) higher magnification.

particles demonstrated some faceting which probably corresponds to fast growth planes during the synthesis process. A high-resolution TEM lattice image of the interface between two crystallites is shown in Figure 4.4 (b). These crystallites can either be individual nanoparticles or extremely small grains that have nucleated separately and joined to form a polycrystalline particle. It appears, however, that these crystallites are mostly individual nanoparticles. TEM analysis of additional RCe sample could resolve the exact order of magnitude of the RCe particle sizes.

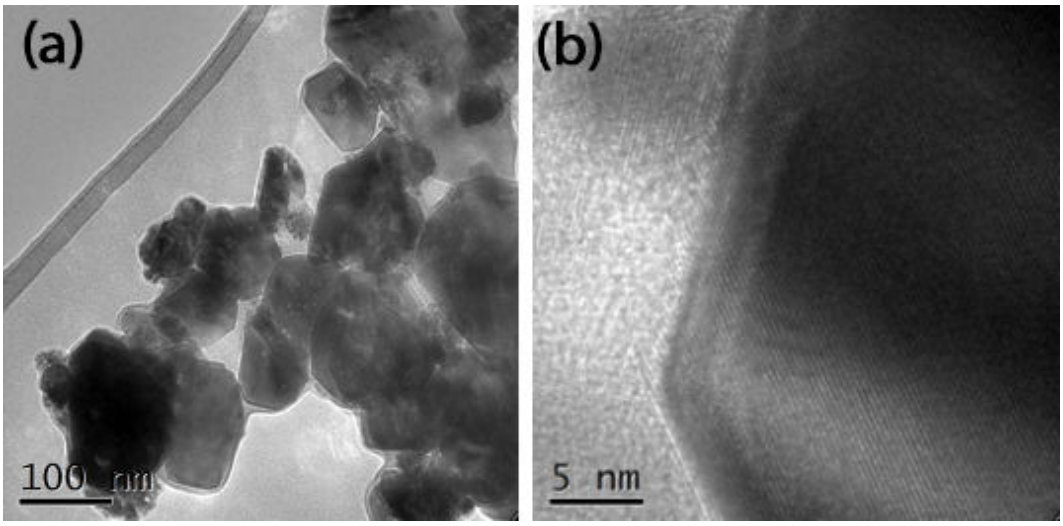

Figure 4.4: TEM analysis of RCe showing (a) particles on the order of 50-100 nm and (b) a high-resolution image of RCe showing a growth facet.

Figure 4.5 shows TEM images of the doped Eu0.5 sample. In Figure 4.5 (a), the variation in the color of the particles comes from the different imaging conditions used. The darker contrast particles are oriented in such a way that they provide strong diffraction contrast when compared to the lighter particles. The magnifications of Figures 4.4 (a)

and 4.5 (a) are very comparable. The comparison clearly shows a significant reduction in particle size in the doped sample (Figure 4.5) when compared to the reference ceria material (Figure 4.4). Figure 4.5 (b) shows a high-resolution image of the crystallite lattice structure. The morphology of the reference ceria and doped ceria samples appear to be similar, both showing faceted surfaces. The doped Ceria samples had a smaller particle/crystallite size of 20 nm, up to 5x smaller than the particle size of the RCe reference ceria provided by LANL. The significantly smaller particle size in the doped ceria powder could lead to an easier propensity to aerosolize and reduce flowability (essentially a "fluffier" powder).

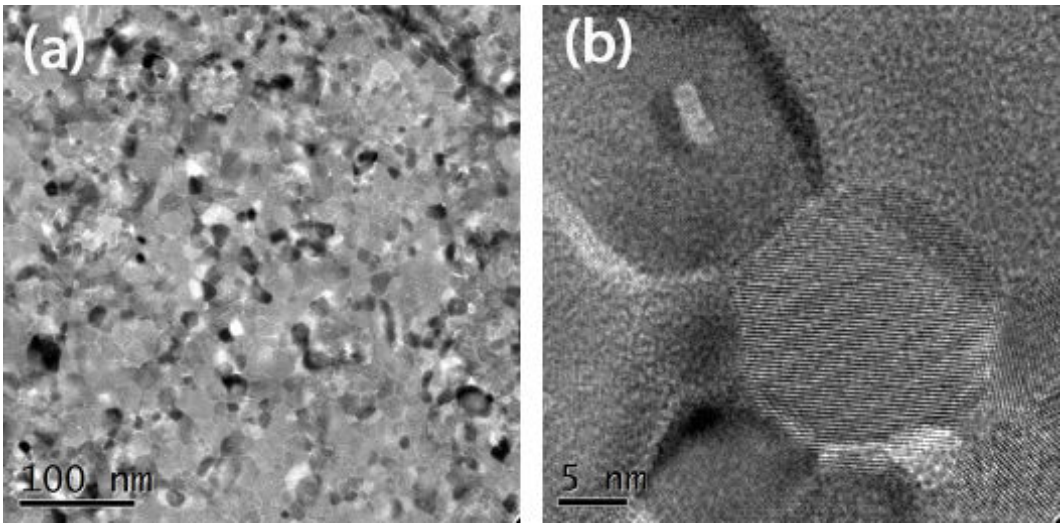

Figure 4.5: Doped Eu0.5 ceria showing (a) particle sizes on the order of 20 nm and (b) high-resolution TEM image of doped Eu0.5 ceria showing small crystallites.

4.2 Brunauer-Emmett-Teller (BET) analysis

BET is the most common method used for determining the surface area of powders. Surface area is calculated as a result of a gas interacting with the surface of the powder being tested. The volume of gas adsorbed to the surface of the particles is measured at the boiling point of the analysis gas. In the present work, nitrogen gas is used, which has a boiling point of -196 °C. It is assumed that the gas condenses on the surface of the particles in a monolayer and as the size of the gas molecule is known the total surface area of the particle is correlated to the volume of gas adsorbed. The equilibrium pressure (p) and saturation pressure (p_0) of the adsorbate at the temperature of adsorption is measured, as well as volume of adsorbed gas (n_a). The surface area of the sample powder is found through the BET equation, Equation 4.1

$$\frac{p}{n_a(p_0-p)}s_{total} = \frac{1}{n_m C} + \frac{(C-1)}{n_m C} * \frac{p}{p_0} \tag{4.1}$$

where n_m is the monolayer capacity, and C is the BET constant. According to BET theory, plotting $\frac{p}{n_a(p_0-p)}$ versus $\frac{p}{p_0}$ should result in a straight line. Using the gradient and

intercept of this line, n_m and C can be calculated according to Equation 4.2 and Equation 4.3:

$$n_m = \frac{1}{gradient + intercept} \tag{4.2}$$

$$C = 1 + \frac{gradient}{intercept} \tag{4.3}$$

Once n_m and C are defined, the total surface area is then given by Equation 4.4

$$s_{total} = \frac{n_m N s}{V} \tag{4.4}$$

where N is Avogadros number, s is the adsorptive cross section of the adsorbing species, and V is the molar volume of adsorbate gas. The extent to which the BET plot is linear determines the confidence with which n_m and C can be calculated. The R^2 of the linear regression is reported as the correlation coefficient. The resulting surface area measurement is reported relative to the mass of the sample, m^2/g.

C relates the degree of adsorbent/adsorbate interaction. A C value less than 20 indicates the BET method is invalid for the material in question. For RCe, C was measured to be 200, and was 956 for the Eu0.5 doped ceria. These values are given in Table 4.1 below.

Table 4.1: Calculated BET constants

Sample	**Calculated BET constant,** C
RCe	200
Eu0.5	956

For calculated BET constants, a C value of 200 is considered to be high or typical. 956 is extremely high, and is likely related to how small the Eu doped ceria particles are. Such a large difference in the calculate C constants indicate that the RCe and Eu0.5 powders are interacting with the N_2 gas in very different ways. BET constant of 200 for the RCe sample would suggest a porous or torturous surface morphology, however this is not supported by TEM analysis which shows similar morphology between the RCe and E0.5 samples with the size being the primary difference. The very high BET constant of 956 for the Eu0.5 sample is possibly due to the very small primary particle size; the BET analysis may not be able to fully distinguish between agglomerates and primary particles at that scale and the agglomerates respond as highly porous particles.

RCe, the LANL supplied ceria, had a measured specific surface area of 13.78 $\pm$ 0.02 m^2/g with a correlation coefficient of 9.999965e-01, while the American Elements 0.5Eu doped ceria was measured to be 13.69 $\pm$ 0.01 m^2/g with a correlation coefficient of 9.999989e-01. These results are tabulated in Table 4.2. As a note, the significant figures of the correlation coefficient are reported by the BET instrument and are important. More 9s in the measurement indicates stronger correlation, and results with 5 9s is considered to be a good measurement.

Table 4.2: BET surface area analysis data.

Sample	Measured specific surface area m^2/g	Correlation coefficient
RCe	13.78 ± 0.02	9.999965e-01
Eu0.5	13.69 ± 0.01	9.999989e-01

The low standard deviation and high correlation factor for both samples indicate a high degree of confidence in the accuracy of the result. Based on BET theory, a smooth spherical particle with the density of ceria at 7.22 g/cm^3 and a surface area of 13.78 m^2/g would have a diameter of 60.3 nm. This is similar, though not identical, to the observed primary particle size of RCe of approximately 100 nm that was identified through TEM analysis. The specific surface area determine by the BET analysis is likely accurate for the RCe sample.

The calculated spherical diameter of Eu0.5 of 60.7 nm varies substantially more from the TEM observations made in the previous section. The TEM analysis in Figure 4.5 shows a particle size for the doped samples around 10 nm. There are several potential explanations for the difference in the particle size results from BET theory and the direct observations made through TEM. It is likely that there is a strong interaction with the absorbate, possibly due to the surface characteristics resulting from the dopant. The interaction of the absorbate along with the very small size is adversely affecting the measurement technique. Additionally, there is little BET data in the literature for particles as small as the Eu doped samples. It is possible that BET theory is breaking down at this scale.

4.3 Tapped Density Results

Powder flowability testing was performed on all of the powders in the present work to describe their respective flowability characteristics. A cylinder with a known amount of material was dropped, or "tapped" until its measured volume remained constant. Based on the measured change in volume and known mass of the sample, an indication of how well the material flowed and packed together is revealed through its change in calculated density.

Table 4.3 shows the data from the experiments that measured the change in volume due to tapping for each of the powders being investigated in this work. The mass of each powder used for the five trials is given in the second column. The remainder of the table reports the averaged bulk volume and its standard deviation for each of the five trials, and the averaged tapped volume and its standard deviation from the five trials. The "bulk volume" is the volume of the powder immediately after it is poured into the graduated cylinder, before any tapping takes place. The "tapped volume" is the measured volume after the cylinder was dropped and a constant volume was observed. For completeness, the raw data for each of the five trials before averaging can be found in Appendix B1. It should be noted that the bulk and tapped volume measurements were made from a graduated cylinder with 0.1 mL markings, and they are less precise than the mass measurements performed on the analytical balance. It was observed that the standard

deviation between the resulting averaged tapped volumes was small, and demonstrated repeatable trials. As the amount of powder used for each sample varied, no other significant conclusions can be drawn from Table 4.3.

Table 4.3: Averaged bulk and tapped volumes of the reference, blended, and doped ceria powders investigated in the present work.

Sample	Measured powder mass (g)	Averaged bulk volume (mL)	Bulk volume std. dev. (mL)	Average tapped volume (mL)	Tapped volume std. dev. (mL)
RCe	2.4935	2.99	0.14	1.89	0.10
A3	3.8501	3.09	0.07	2.36	0.05
A4	5.01	4.23	0.14	2.98	0.03
B3	3.8956	3.71	0.05	2.45	0.00
B4	3.3126	3.38	0.08	2.09	0.07
C3	3.8599	3.55	0.05	2.47	0.03
C4	2.9021	3.18	0.10	1.98	0.03
Eu0.5	0.4185	4.85	0.10	2.84	0.04
Eu1	0.2522	3.30	0.04	2.11	0.09
Eu2	0.3007	4.51	0.04	2.66	0.05

Using the data presented in Table 4.3, Table 4.4 reports the calculated bulk (pre-tapping) and tapped densities of the various powders. Additionally, Table 4.4 records a normalized value for each bulk and tapped density, calculated as a % of the measured bulk and tapped density to the theoretical density of ceria (7.215 g/cc) and plutonium oxide (11.5 g/cc), respectively. The calculated values with respect to the theoretical bulk density of plutonium oxide were performed to show a general comparison of each powder sample to plutonium oxide.

Table 4.4: Calculated bulk and tapped densities of each powder sample.

Sample	Bulk (g/cc)	Bulk % of ceria density	Bulk % of PuO_2 density	Tapped (g/cc)	Tapped % of ceria density	Tapped % of PuO_2 density
Ce	0.835	12	7.3	1.32	18	11
A3	1.25	17	11	1.63	23	14
A4	1.19	16	10	1.68	23	15
B3	1.05	15	9.1	1.59	22	14
B4	0.98	14	9	1.59	22	14
C3	1.09	15	9.5	1.56	22	14
C4	0.913	13	8	1.47	20	13
Eu0.5	0.086	1.2	0.75	0.147	2	1.3
Eu1	0.076	1.1	0.66	0.12	1.7	1
Eu2	0.067	1	0.6	0.113	1.6	1

In general, the results in Table 4.4 showed that the addition of the commercial phos-

phors to the blended samples, A3, A4, B3, B4, C3, and C4, increased both the bulk density and the resulting tapped density with respect to the reference ceria powder, RCe. This is likely due to the multiple particle sizes in the blended samples. One of the properties of powders is that their packing density can change substantially with even small additions of new modes to the particle size distribution. Conversely, the doped samples, Eu0.5, Eu1, and Eu2, all measured a lower tapped density than the reference powder RCe, by an order of magnitude. It is also observed that the tapped density of the doped powders decreases as the doping concentration increases from 0.5-2.0%. The lower measured tapped densities correspond to the less agglomerated, lower density structure of the doped samples that was observed during the FE-SEM analysis.

The data presented in Table 4.4 were further used to quantify the relationship between the flowability of the powders though the Hausner Ratio and Carr's compressibility index [2, 3]. The Hausner Ratio (HR), a ratio of the tapped density to the bulk density, is defined by Equation 4.5 [3]:

$$HR = \frac{\rho_t}{\rho_b} \tag{4.5}$$

where ρ_t is the measured tapped density of the powder, and ρ_b is the measured bulk density [3]. A powder having an HR of greater than 1.35 indicates that it is a material with poor flowability. Carr's compressibility index (CI), a second quantitative measure for comparing flowability of powder is given by Equation 4.6 [3]:

$$CI = 100(1 - \frac{\rho_b}{\rho_t}) \tag{4.6}$$

Table 4.5 below compares the calculated HR and CI values to flow characteristics of the powder samples [4].

Table 4.5: General scale of flowability for powders, comparing the Hausner Ratio and Carr's Compressibility Index

Hausner Ratio (HR)	**Flow Character**	**Carr's Compressibility Index (CI, %)**
1.00-1.11	Excellent	< 11
1.12-1.18	Good	11-15
1.19-1.25	Fair	16-20
1.26-1.34	Passable	21-25
1.35-1.45	Poor	26-31
1.46-1.59	Very poor	32-37
> 1.60	Very, very poor	> 38

Table 4.5 demonstrates that powders have fair to good flowability with a HR less than 1.35 and a CI less than 25. Table 4.6 presents both the experimental HR and CI for all of the powders studied in the present work: RCe, A3, A4, B3, B4, C3, C4, Eu0.5, Eu1, and Eu2. Results are compared to measurements of various PuO_2 samples either provided

by LANL through email communication (Air Hatch Material), or listed in the paper by Wayne et al. [2]. The work by Wayne et al. characterized PuO_2 powder oxidized by different methods in different years: Advanced Recovery and Integrated Extraction System, ARIES, (AR), muffle furnace oxidation (MF), and ARIES production, fully processed (UPOP). The "Air Hatch Material" sample was investigated by Josh Narlesky at LANL specifically for the purposes of comparison to the ceria sample characterized in this work. The authors of the report thank Mr. Narlesky for the time spent performing the experiments, and for providing valuable comparison data to this project.[1]

Table 4.6: Experimental Hausner Ratio (HR) and Carr's compressibility index (CI) for the ceria powders studied in the present work, compared to PuO_2 values from Wayne et al. [2]

Powder	**Hausner Ratio (HR)**	**Carr's Compressibility Index (CI, %)**
RCe	1.58	36.8
A3	1.31	23.6
A4	1.42	29.5
B3	1.51	33.9
B4	1.62	38.2
C3	1.44	30.4
C4	1.61	37.7
Eu0.5	1.71	41.4
Eu1	1.57	36.1
Eu2	1.7	41
Hatch Material (air oxidized metal) ref: J. Narlesky, LANL	1.29	22.2
AR (2009-07-09) not processed or calcined [2]	1.16	13.4
AR (2009-07-14/2009-07-15) [2]	1.14	11.9
AR (2009-07-23/2009-07-29) not processed or calcined [2]	1.22	17.7
MF (2012-08-08/2012-09-19) not processed [2]	1.2	15.9
UPOP (2010-07-20/2011-08-20) [2]	1.21	17.4
UPOP (2012-01-24/2012-09-06) [2]	1.23	18.4
MF (2012-09-24) fully processed [2]	1.28	21.8
UPOP (2012-09-24/2013-04-17) [2]	1.3	23.4

For the ceria powders analyzed in the present work, all samples with the exception of A3 exhibit poor flowability based on the HR and the CI. A3 falls into the "passable" flow category. Specifically, the doped ceria powders, Eu0.5, Eu1, and Eu2 fall into the "very, very poor" flowability characterization. The PuO_2 powders from Wayne et al. [2] range from "good" flowability to "passable" flowability on both scales. In general, the PuO_2 powders demonstrate relatively better flowability characteristics than the simulant

[1]The authors also acknowledge Kirk Veirs, Murray Moore, and Laura Worl for guiding the hatch material experiments and overseeing the safe handling of plutonium during the bulk and tapped density experiments.

ceria powders based on the HR and CI scales. This difference in observed flowability is an expected result, as the ceria production process is different than that of the PuO_2. The blended ceria samples produced from commercial phosphor G525, A3 and A4, show a similar flowability to the Hatch Material PuO_2, MF fully processed PuO_2, and UPOP PuO_2.

Within the experiments performed at NMT, it is observed that decreasing the amount of commercial phosphor, i.e., going from A3 to A4, B3 to B4, etc, decreases the flowability of the blended samples. Like with the volume measurements, this is likely due to the multiple particle sizes in the blended samples. Since a powders packing density can change substantially with even small additions of new modes to the particle size distribution, increasing the amount of the larger particle size has increased the powders flowability. Both the flowability and density of blended samples are similar to reference ceria, indicating that the addition of the commercial phosphor does not significantly change the "poor" flowability of the reference sample. The doped samples are consistently observed to have less flowability than the blended samples, which is likely linked to the process used to synthesize the doped samples. Also the average particle size is significantly smaller than the reference ceria sample which would contribute to lower flowability (assuming similar particle morphology).

The tapped density values calculated in the present work are presented graphically in Figure 4.6 and compared to the PuO_2 data from Wayne et al. [2]. Figure 4.6 is similar to an Ashby plot because it displays multiple materials properties on the same figure, i.e., calculated tapped density as a function of calculated bulk density. Since flowability is related to the ratio of densities through the Hasuner Ratio in Equation 4.5, each point on the graph is a visual representation of the flowability for a single sample powder. Additionally, the results in Figure 4.6 are compared to a line of HR=1.35.

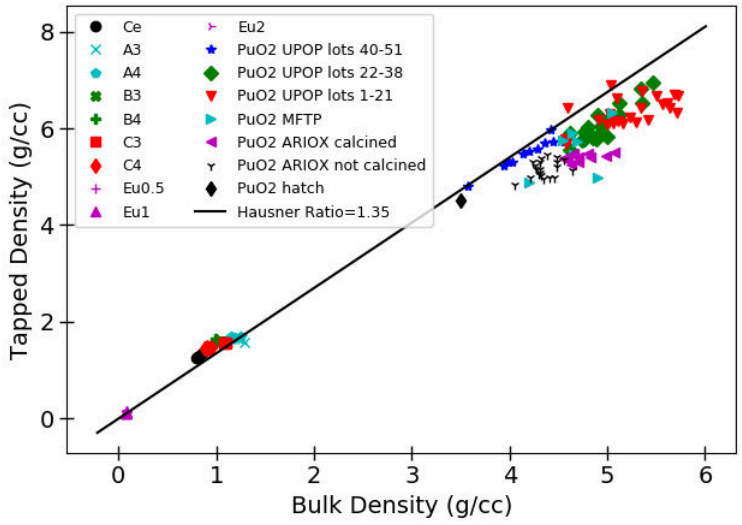

Figure 4.6: Calculated tapped verses bulk density of the powders examined in the present work compared to known PuO_2 values and plotted with a Hausner Ratio of 1.35.

The HR line of 1.35 represents the boundary between "passable" and "poor" flowability of the material, where material with an HR < 1.35 demonstrate "passable" flow

characteristics. On Figure 4.6, the powders that exhibit "passable" flow will fall below the black line of HR=1.35. In general, almost all of the PuO_2 powders exhibit "passable" flow, with the exception with some of the samples from the UPOP lots 1-21. Conversely, reference ceria, RCe, and all of the blended powders with the exception of A3, fall above the line, thus demonstrating "poor" flow characteristics. Blended sample A3 falls above the HR line of 1.35. The doped sample, clustered in the bottom left of the plot, should lie above the line, but the scaling of the plot make it difficult to discern their locations.

4.4 UV-Vis Spectroscopy Results

Ultra-violet and visible spectroscopy (UV-Vis) testing was performed on all 13 samples examined in the present work. The purpose of UV-Vis testing is to determine the actual absorption peak for each of the luminescent materials, and determine how much the reported absorption differs from the actual, measured absorption peak.

First, UV-Vis testing was performed on the pure commercial phosphor samples: A1, B1, and C1. Figure 4.7 shows the UV-Vis absorption over 300 - 800 nm for A1 (black line), B1 (blue line), and C1 (red line) commercial phosphors. It should be noted that the vertical axis of Figure 4.7 is normalized so that the maximum measured absorption in each test has a value of 1.0. and presented in dimensionless units to accommodate all three samples on one plot. The peaks in the absorption plot (shown between 400 - 500 nm for these samples) represent the actual wavelength of light that the phosphor absorbs. Additionally, the A1, B1, and C1 samples all absorb a secondary peak around 350 nm. This extra peak is likely due to another absorption energy from the YAG structure itself.

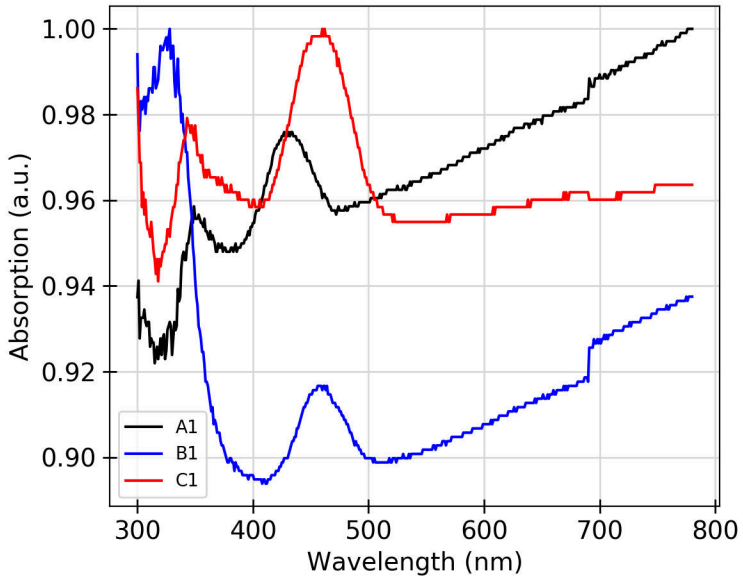

Figure 4.7: UV-Vis absorption spectra for commercial phosphor samples: A1 (black line), B1 (blue line), and C1 (red line). The absorption (vertical axis) values are presented in arbitrary units.

The reported absorption ranges for the commercial phosphors are tabulated in Table

4.7. All three commercial phosphor samples, A1, B1, and C1, showed absorption peaks within reported ranges.

Table 4.7: Reported absorption ranges for the commercial phosphors compared to the measured peak in the present work

Phosphor	Commercial Name	Reported absorption range	Measured absorption peak center (this work)
A1	G525	420 - 460 nm	438 nm
B1	Y550	430 - 480 nm	464 nm
C1	Y570	440 - 490 nm	462 nm

After confirming that the commercial phosphors absorbed in their reported ranges, the blended samples A3, A4, B2, B4, C3, and C4 were tested and compared to the reference ceria, Ce. Figure 4.8 shows a plot of all 6 blended samples, A3 (gold line), A4 (blue line), B3 (red line), B4 (green line), C3 (purple line), C4 (aquamarine line), compared to Ce (black line) reference ceria. Again, it should be noted that the absorption data are normalized so the maximum absorption takes on a value of 1.0 to accommodate all seven results on one plot. It is clear from examination of the Figure 4.8 that the absorption spectra of the blended samples were dominated by ceria absorption. The absorption peaks of the phosphors that were identified in Figure 4.7 were not distinguishable from the ceria peak. The presence of the commercial phosphor did create a broadening of the absorption peak in all 6 blended samples compared to the reference sample. No notable correlations exist between the effect of the amount of commercial phosphor (2.5 vs 5 wt %) and the absorption spectra results presented in Figure 4.8.

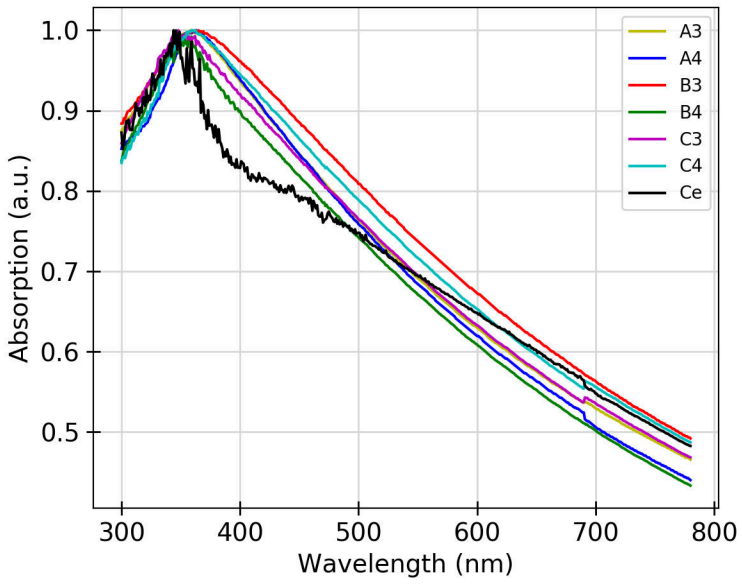

Figure 4.8: UV-Vis absorption of blended samples: A3 (gold line), A4 (blue line), B3 (red line), B4 (green line), C3 (purple line), C4 (aquamarine line) compared to the absorption spectra of RCe (black line) reference ceria.

Finally, UV-Vis was performed on the 3 doped samples: Eu0.5, Eu1, and Eu2. The europium doping in the ceria microstructure is intended to distort the symmetry of ceria's crystal structure in order to allow the ceria to absorb the light more efficiently. It should be noted that the presence of europium should not affect the absorption spectra of the Eu0.5, Eu1, or Eu2 samples. Hence, UV-Vis was performed on the doped samples to confirm that their absorption spectra was similar to that of the reference ceria. A plot of the absorption spectra results is presented in Figure 4.9, where the Eu0.5 is the black line, Eu1 is the blue line, and Eu2 is the red line. The absorption intensities presented in Figure 4.9 have been normalized so that the peak absorption takes on a value of 1.0 to accommodate all three results on one plot. The results in Figure 4.9 confirm that the absorption range of the three doped ceria samples has not been altered from the absorption range of the RCe in Figure 4.8.

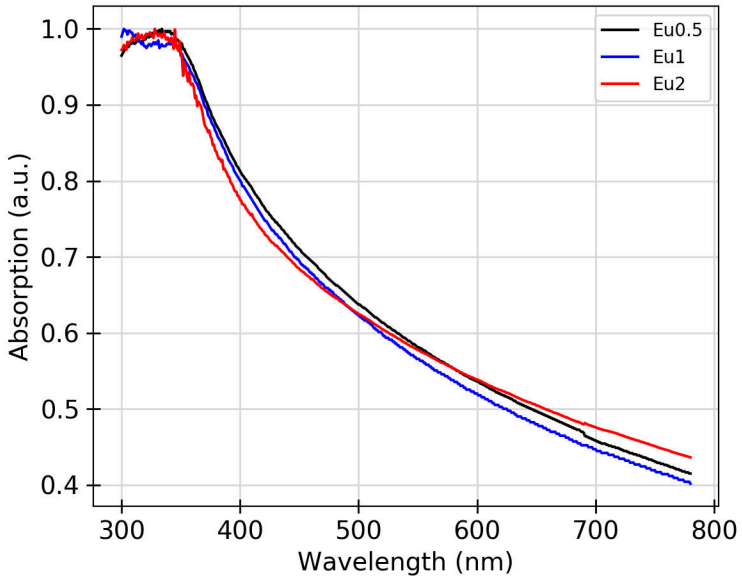

Figure 4.9: UV-Vis absorption of doped samples: Eu0.5 (black line), Eu1 (blue line), and Eu2 (red line).

4.5 Flourospectroscopy Testing Results

Flourospectroscopy was performed on all 13 of the powder samples being investigated in the present work. The goal of flourospectroscopy is to determine the exact emission spectra for the pure commercial phosphors, the blended ceria samples, and the doped ceria samples when they have been excited with their measured peak absorption wavelength determined from the UV-Vis experiments. The excitation wavelength for each powder sample is given in Table 4.8 below. Slit width for excitation was maintained at 5 nm, such that an excitation wavelength $\pm$ 2.5 nm was used.

For all of the results presented in this section, the emission spectra of the baseline powder-free PDMS in the polystyrene cuvette was subtracted from the data produced by the spectroflourophotometer for the excitation wavelength corresponding to the values

Table 4.8: Excitation wavelength for each powder sample used in flourospectroscopy. Slit width was maintained at 5 nm.

Sample	Flourospectroscopy excitation wavelength (nm $\pm$ 2.5 nm)
RCe	350
A1, A3, A4	425
B1, B3, B4	470
C1, C3, C4	460
Eu0.5, Eu1, Eu2	355

in Table 4.8. The emission spectra for the baseline runs are presented in Appendix C1. Unless otherwise noted, the emission spectra were normalized based on the powder mass used for each individual sample. Thus, the vertical axes in Figures 4.10 are presented in arbitrary, normalized units.

First, flourospectroscopy was performed on the pure commercial phosphor samples: A1, B1, and C1. Figure 4.10 shows normalized emission intensity as a function of wavelength for the samples: A1 (black line), B1 (blue line), and C1 (red line).

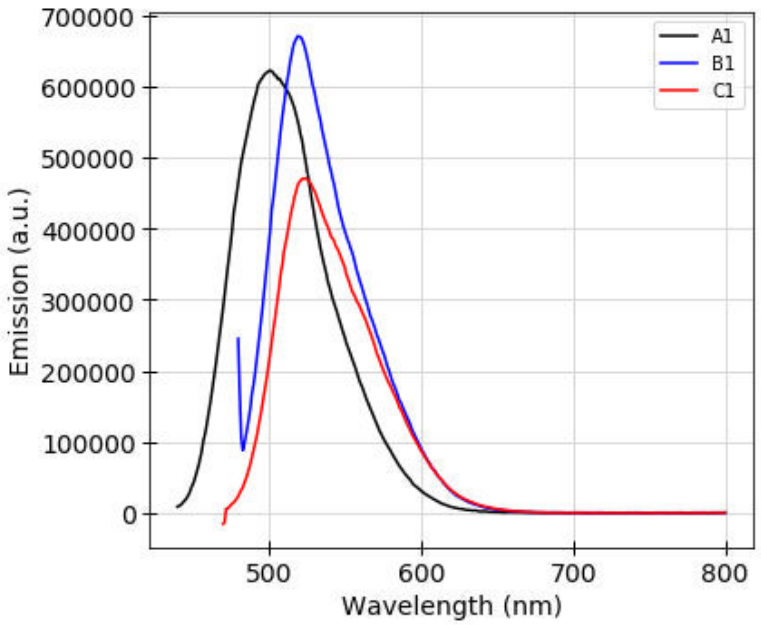

Figure 4.10: Flourospectroscopy emission spectra for commercial phosphor samples: A1 (black line), B1 (blue line), and C1 (red line). The emission (vertical axis) values are normalized by sample mass and presented in arbitrary units.

The emission spectra for each of the commercial phosphors shown in Figure 4.10 peaked at a lower wavelength than their reported value. The reported emission values are presented in Table 4.9 and compared to the measured emission values from this present work. The difference was about 25 nm for A1 and B1, and about 50 nm for C1. The spectroflourophotometer used for these tests was calibrated upon its installation in the

Chemistry Department at New Mexico Tech. The machine runs a self-calibration before each scan, and it was determined that the calibration of the machine was not the source of the measured emitted peak shift for these commercial phosphors. Further investigation into this shift did not provide insight into why it occurred.

Table 4.9: Reported emission value for the commercial phosphors.

Phosphor	Commercial Name	Reported emission value	Measured emitted peak center (this work)
A1	G525	525 nm	501 nm
B1	Y550	550 nm	519 nm
C1	Y570	570 nm	524 nm

After characterizing the commercial phosphors, the emission of the blended samples A3, A4, B3, B4, C3, and C4 were examined. Figure 4.11 shows a plot of all 6 blended samples: A3 (gold line), A4 (blue line), B3 (red line), B4 (green line), C3 (purple line), C4 (aquamarine line), compared to the emission of RCe (black line) reference ceria. Note that the data in Figure 4.11 was not normalized to mass. Since the sample results were not normalized to mass, the emission wavelength is the most important feature of Figure 4.11 for each sample shown. The tall peaks present in all six blended samples below 500 nm can be disregarded. The authors believe that the variation in the tall peaks is a scattering effect at lower wavelengths resulting from an interaction of the cuvette itself, the PDMS, and the phosphor and RCe powders.

As expected, almost no difference is observed in the emission peak between samples that contain the same commercial phosphor for commercial phosphors A and B. For example, A3 and A4 have emission peaks at 495 nm, and B3 and B4 have emission peaks around 520 nm. Furthermore, A3, A4, B3, and B4 samples show emission peaks similar to measurements on their respective pure phosphor samples presented in Figure 4.10 and Table 4.9. The C4 sample shows a downshift in emission spectra by approximately 20 nm when compared with its pure phosphor counterpart, creating a variation in the emission peak between C3 and C4. The cause for this is difference in the C3 and C4 samples is unknown. The reference ceria sample, RCe, shows no emission, as no luminescent materials are present.

Finally, flourospectroscopy was performed on the doped samples: Eu0.5, Eu1, and Eu2. Figure 4.12 shows a normalized plot of the resulting emission spectra with the Eu0.5 (black line), Eu1 (blue line), and Eu2 (red line). The results in Figure 4.12 were normalized to the mass of the powder used in the sample. The emission data for the doped sample show excellent agreement to the reported emission value of 592 nm. As a reminder, the doped ceria samples show photoluminescence properties, whereas the reference ceria provided by LANL in Figure 4.10 does not. The europium doping int he microstructure changes the ability of the ceria structure to emit light.

Since the A.U. of the y-axis in Figure 4.10 is consistent between samples run with the flourospectrometer, normalizing the results to weight allows for a direct comparison between the strength of the emission wavelength. The Eu2 sample, which is comprised of 2 weight% europium, shows a reduction in emission strength compared to the Eu0.5 and

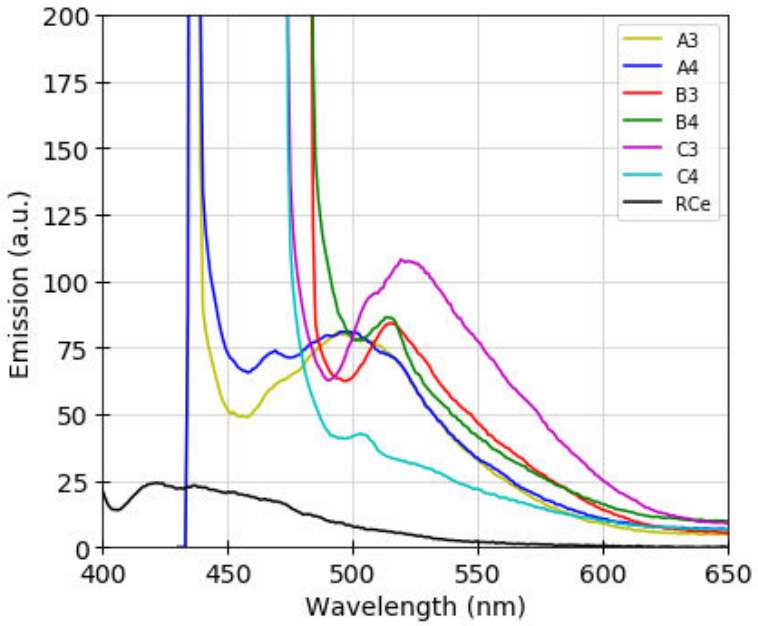

Figure 4.11: Flourospectroscopy emission of blended samples: A3 (gold line), A4 (blue line), B3 (red line), B4 (green line), C3 (purple line), C4 (aquamarine line) compared to the emission spectra of RCe (black line) reference ceria. This data set is not normalized.

Eu1 sample. This reduction in emission strength corresponds to quenching, or the saturation point, of the fluorescence effect at this weight % dopant in the ceria microstructure. As mentioned previously, the purpose of doping the ceria with europium is to perturb its symmetry and enhance its absorption and emission spectra. At some point, the doping becomes less effective and this is known as the quenching point. In conclusion, the Eu1 sample is the maximum emission intensity for europium doped ceria. This is expected, as there is always a maximum doping percentage for these types of materials.

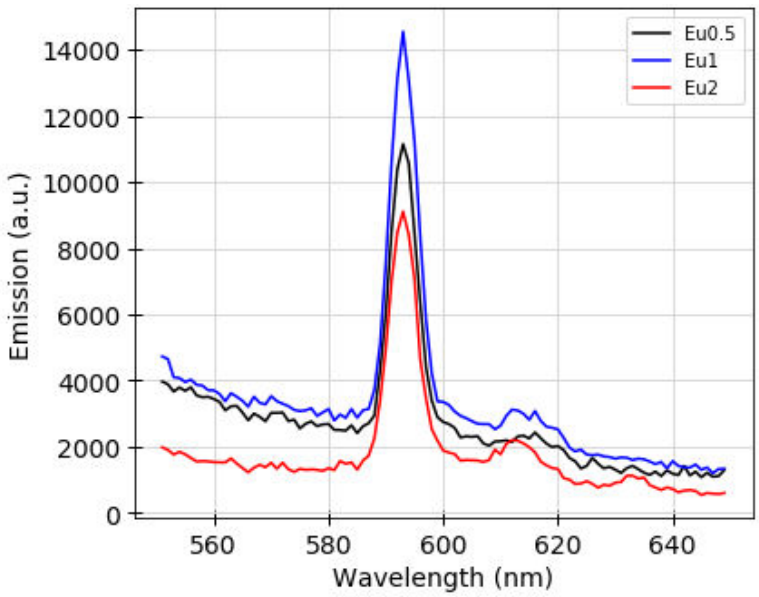

Figure 4.12: Flourospectroscopy results for the doped samples: Eu0.5 (black line), Eu1 (blue line), and Eu2 (red line). All samples are normalized by powder mass.

5 Conclusions

Key findings from this project include:

1. Optical microscopy, scanning electron microscopy, and transmission electron microscopy were used to determine approximate particle sizes of the LANL reference ceria and the doped ceria powder purchased from American Elements. For all powders, the particle sizes were reported by the manufacturer to be less than 1 μm. The SEM work proved that the majority of the ceria particle were substantially smaller than reported by the manufacturers. The TEM analysis showed particle sizes for the reference ceria to be on the order of 50-100 nm, and particles sizes for the doped ceria to be on the order of 20 nm. The doped ceria produced by American Elements has particles sizes up to an an order of magnitude smaller than the reference ceria used at LANL.

2. BET analysis was performed to measure the surface area of the reference ceria provided by LANL and the 0.5 wt% europium doped ceria. Both powders examined measure similar specific surface area. The particle size of the reference ceria observed from TEM was similar to that calculated using BET theory, while the particle size of the doped ceria calculated with BET theory varied substantially from the TEM observations. This is likely due to the interaction of the dopant with the absorbate used in BET. It could also be due to breakdown of BET theory at this small scale, or other factors such as surface charge or surface roughness that were not observed by the scope of the present test methods.

3. Flowability testing of all powders was performed through tapped density experiments. Tapped density experiments calculate the density of a powder after it has

been "tapped" down to a constant volume. With the exception of the A3 powder, the reference ceria, ceria powders blended with commercial phosphor, and europium doped ceria all demonstrated "poor" to "very, very poor" flowability based on calculated Hausner Ratio or Carr's Compressibility Index. The doped samples had "very, very poor" flowability, likely due to their smaller particle size compared to the reference ceria. When compared to tapped density results from seven types of PuO_2 powders previously published by LANL, the blended and doped ceria powders displayed poorer flowability.

4. UV-Vis Spectroscopy was performed on all powder samples studied in the present work to determine the luminescent absorption peak. The pure commercial phosphors yielded measured absorption peaks within the reported range from the manufacturer. In the case of the blended powders, the absorption peaks were dominated by the absorption peak of pure ceria, though the presence of the phosphor broadened the absorption peak in all cases. UV-Vis was performed on the doped sample and showed that the presence of the europium dopant did not alter the measured absorption peak of the ceria.

5. Flourospectroscopy testing was performed on all of the powder samples studied in the present work using an excitation wavelength as determined from the UV-Vis results. The pure commercial phosphor all produced measured emitted peak centers 20-30 nm lower than the emission value reported by the manufacturer. No reason for this shift was identified, as recent flourospectrometer calibration yielded consistent results. The A3, A4, B3, and B4 blended powders showed emission peaks consistent with their pure commercial phosphors, while the C3 and C4 powders showed further downshift in the emission peaks. As expected, the reference ceria did not emit. Flourospectroscopy of the doped ceria powders yielded self-consistent results confirming the emission peak reported by the manufacturer. The results indicate the quenching point for europium in the ceria microstructure is somewhere between 1 and 2 wt% europium.

6 Recommendations

Two conclusions from the experiments performed in the present work comparing undoped reference ceria provided by LANL and the europium doped ceria purchased from American elements were made: (1) the doped ceria is detectable due to its photoluminescent properties (2) the synthesis technique of the doped ceria yields particle sizes that are an order of magnitude smaller than the reference ceria. Based on these conclusions, the following recommendations can be made:

- Further investigation of the properties of reference ceria versus doped ceria.
  - Investigation of the particle size distributions of the reference ceria and doped ceria could yield further information on the flowability potential of these powders. Bi- or tri-modal particle sizes increase the ability of the powder to pack, and in turn, increase its flowability.

  - X-ray diffraction linewidths have been used to estimate crystallize sizes in PuO_2. Crystallite sizes are different from particle sizes and some of the subtleties between individual particles (which are best described as crystallites) and agglomerates (more like particles as measured by a particle size instrument) may be elucidated using this technique. This would be particularly useful to investigate if crystallite sizes of the RCe are sub 10 nm.
  - Develop a test to determine the ease of release of the doped ceria versus reference ceria from a transient pressurization event in a PuO_2 containment system.
  - Develop the optical characterization technique for detection of the location of an in-situ particle release from a pressurized PuO_2 containment system.
  - Compare the "dustiness" of the various ceria surrogate materials to the "dustiness" of PuO_2 powders. The respirable "dustiness" is algebraically identical to the respirable release fraction (RRF), where the standard defines the manner of powder dispersal (e.g. powder falling through a vertical tower, or dispersed from a rotating drum).

- Perform identical experiments to those performed in the present work on un-doped ceria. This un-doped ceria would be made from the same synthesis procedure used for the doped ceria samples Eu0.5, Eu1, and Eu2. These proposed experiments would separate the effects of the synthesis method from the presence of the dopant on the resulting powder properties.

- Perform drop tests on a PuO_2 containment system to determine the ease of release of the doped ceria powders through the filter, or other components of the container.

- Apply the characterization method outlined in this document to other PuO_2 surrogate materials relevant to work at LANL. For example, TiO_2 with sodium fluorescein tracers could be investigated.

7 Acknowledgements

This work was funded by LANL Subcontract No. 499434. These funds, in part, supported Joshua Strother and Kristin Mackowski, the graduate students who performed the majority of the experimental work on this project. The authors would like to acknowledge their time and effort spent to complete this work. The authors would also like to acknowledge Dr. Ying-Bing Jiang from the University of New Mexicos Center for Micro-Engineered Materials for performing the TEM analysis.

Appendix A Calibration of the spectroflourphotometer

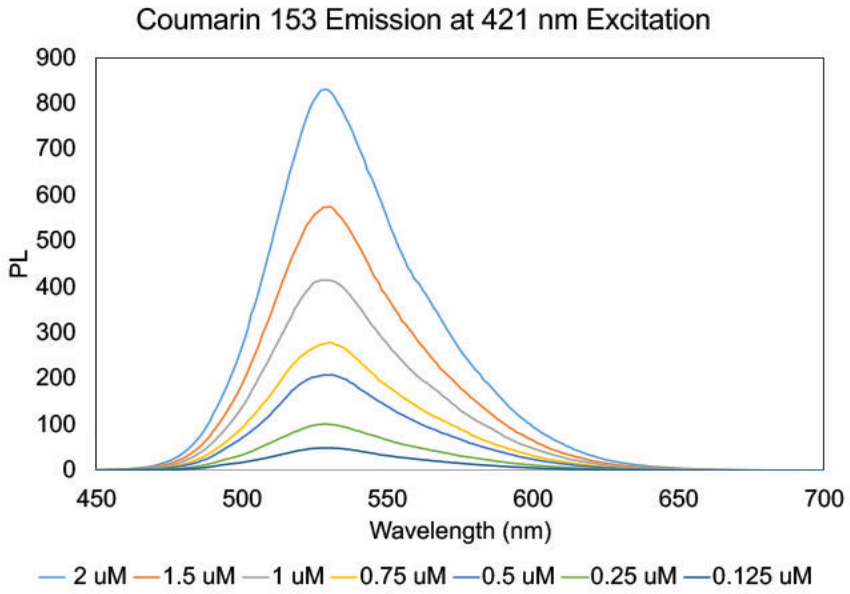

Figure A1: Spectroflourophotometer calibration curves of coumarin 153 dye in an ethanol solvent ranging from 0.125 uM - 2 uM.

Appendix B Tapped volume raw data

Table B1: Bulk and tapped volume raw data for the 10 powders studied. The measured values for all five trials are presented along with their average and standard deviation values.

Sample	Volume (mL)	Trial #1 (mL)	Trial #2 (mL)	Trial #3 (mL)	Trial #4 (mL)	Trial #5 (mL)	Ave. (mL)	Std. Dev. (mL)
RCe	Bulk	3.15	3.1	3	2.9	2.8	2.99	0.14
	Tapped	2	1.95	1.9	1.85	1.75	1.89	0.1
A3	Bulk	3	3.05	3.1	3.15	3.15	3.09	0.07
	Tapped	2.45	2.35	2.3	2.35	2.35	2.36	0.05
A4	Bulk	4	4.3	4.2	4.3	4.35	4.23	0.14
	Tapped	2.95	3	3	3	2.95	2.98	0.03
B3	Bulk	3.7	3.7	3.7	3.8	3.65	3.71	0.05
	Tapped	2.45	2.45	2.45	2.45	2.45	2.45	0
B4	Bulk	3.5	3.35	3.4	3.35	3.3	3.38	0.08
	Tapped	2.2	2.1	2.1	2	2.05	2.09	0.07
C3	Bulk	3.6	3.5	3.5	3.55	3.6	3.55	0.05
	Tapped	2.45	2.45	2.5	2.45	2.5	2.47	0.03
C4	Bulk	3.3	3.2	3.25	3.1	3.05	3.18	0.1
	Tapped	2	1.95	2	2	1.95	1.98	0.03
Eu0.5	Bulk	5	4.8	4.9	4.75	4.8	4.85	0.1
	Tapped	2.85	2.9	2.8	2.8	2.85	2.84	0.04
Eu1	Bulk	3.35	3.3	3.25	3.3	3.3	3.3	0.04
	Tapped	2.25	2.1	2	2.1	2.1	2.11	0.09
Eu2	Bulk	4.5	4.55	4.5	4.45	4.55	4.51	0.04
	Tapped	2.6	2.7	2.6	2.7	2.7	2.66	0.05

Appendix C Flourospectroscopy of powder-free PDMS in a polystyrene cuvette.

Figure C1 shows the flourospectroscopy results of a powder-free PDMS sample in a polystyrene cuvette excited under wavelengths of (a) 355 nm, (b) 425 nm, (c) 460 nm, and (d) 470 nm. The PDMS shows an emission peak around 720 nm when excited at wavelengths less than 400 nm. Also note the artifact in the data present at lower wavelengths.

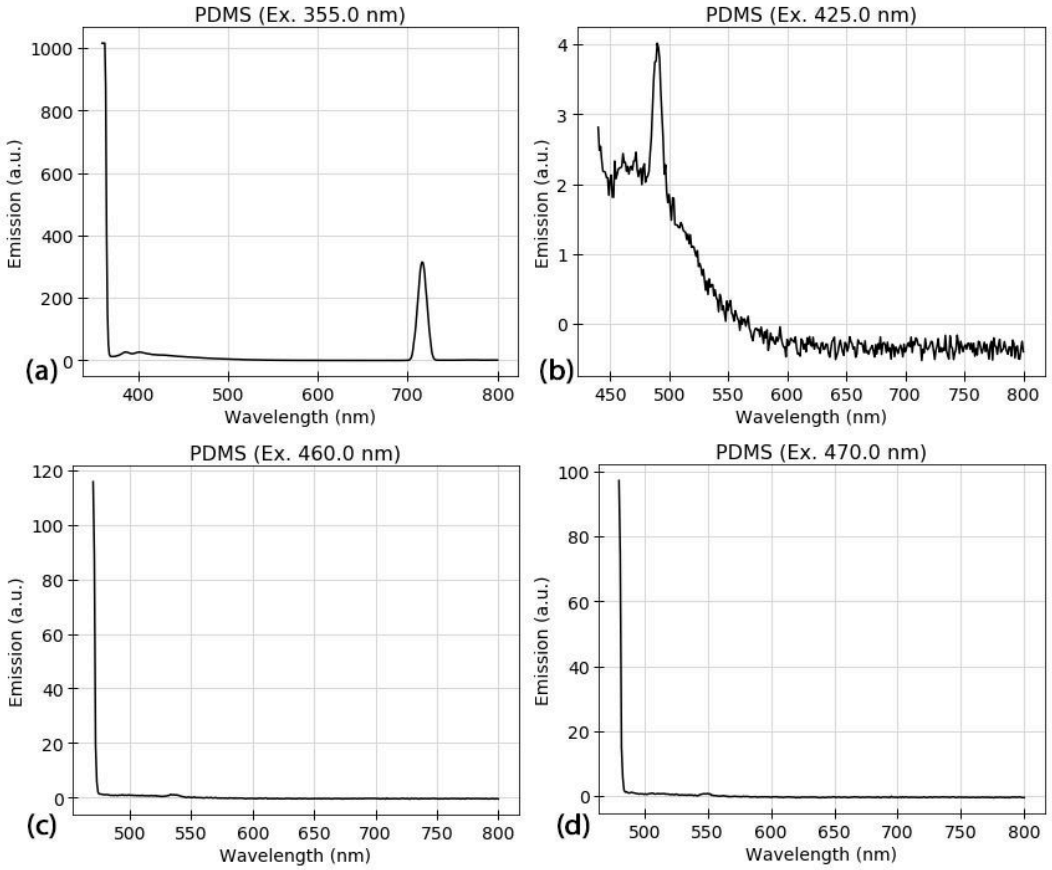

Figure C1: Flourospectroscopy of a powder-free PDMS sample in a polystyrene cuvette excited at (a) 355 nm, (b) 425 nm, (c) 460 nm, and (d) 470 nm.

References

[1] G. Vimal, Kamal P. Mani, P. R. Biju, Cyriac Joseph, N. V. Unnikrishnan, and M. A. Ittyachen. Structural studies and luminescence properties of CeO2:Eu3+ nanophosphors synthesized by oxalate precursor method. *Applied Nanoscience*, 5(7):837–846, oct 2015.

[2] David M. Wayne, Larry G. Peppers, Daniel S. Schwartz, and Paul C. DeBurgomaster. Surface area and particle size distribution of plutonium oxides derived from the direct oxidation of Pu metal. *Journal of Nuclear Materials*, 511:242–263, dec 2018.

[3] Nayland Stanley-Wood. Bulk Powder Properties: Instrumentation and Techniques. In *Bulk Solids Handling*, pages 1–67. Blackwell Publishing Ltd., Oxford, UK.

[4] R. L. Carr. Evaluating Flow Properties of Solids. *Chemical Engineering Journal*, 72:163–168, 1965.